Acta Crystallographica Section D
Biological Crystallography
ISSN 0907-4449

Third calcium ion found in an inhibitor-bound phospholipase A_2

K. Sekar,[a,b]* D. Gayathri,[c] D. Velmurugan,[c] J. Jeyakanthan,[a] T. Yamane,[d] M.-J. Poi[e] and M.-D. Tsai[e,f]

[a]Bioinformatics Centre, Indian Institute of Science, Bangalore 560 012, India, [b]Supercomputer Education and Research Centre, Indian Institute of Science, Bangalore 560 012, India, [c]Department of Crystallography and Biophysics, University of Madras, Guindy Campus, Chennai 600 025, India, [d]Department of Biotechnology and Biomaterial Science, Graduate School of Engineering, Nagoya University, Furo-cho, Chikusa-ku, Nagoya 464-8603, Japan, [e]Departments of Chemistry and Biochemistry and The Ohio State Biochemistry Program, The Ohio State University, Columbus, OH 43210, USA, and [f]Genomics Research Centre, Academia Sinica, Taiwan

Correspondence e-mail: sekar@physics.iisc.ernet.in, sekar@serc.iisc.ernet.in

Received 8 December 2005
Accepted 14 January 2006

PDB Reference:
K53,56,121M PLA_2–anisic acid complex, 2b96, r2b96sf.

The lipolytic enzyme phospholipase A_2 plays a crucial role in lipid metabolism and catalyzes hydrolysis of the fatty-acid ester bond at the *sn*-2 position of phospholipids. Here, the crystal structure (1.7 Å resolution) of the triple mutant (K53,56,121M) of bovine pancreatic phospholipase A_2 complexed with an organic molecule, *p*-methoxybenzoic acid (anisic acid), is reported. Residues 60–70 (the surface-loop residues) are ordered and adopt conformations which are different from those normally found in structures in which a second calcium ion is present. It is interesting to note that for the first time a third calcium ion has been identified. In addition, four Tris (2-amino-2-hydroxymethyl-1,3-propanediol) molecules were located. It is believed that one of the Tris molecules plays a role in clamping the third calcium ion and that another is involved in controlling the dynamics of the surface loop through hydrogen bonds.

1. Introduction

Phospholipase A_2 (PLA_2; EC 3.1.1.4), one of the most intensively studied proteins, is a hydrolytic calcium-dependent enzyme. PLA_2 is found both inside and outside the cell. PLA_2s are classified into two families, extracellular ($sPLA_2$s) and intracellular ($cPLA_2$s), and are further divided into various groups based on molecular weight, amino-acid sequence, substrate specificity and disulfide-bond pattern. Extracellular/secretory PLA_2s ($sPLA_2$s) are easy to isolate and have therefore been studied the most. Intracellular PLA_2s, which are normally bound to the membranes, are less easy to isolate. Groups IA (cobras and kraits, 13–15 kDa), IB (mammalian pancreas and spleen, 13–15 kDa), IIA (mammalian platelets, 13–15 kDa), IIB (rattlesnakes and vipers, 13–15 kDa), IIC (rat/mouse testis, 15 kDa), III (insects, lizards and mammals, 16–18 kDa), V (human/rat/mouse macrophages and lung, 14 kDa), VII (human plasma, 45 kDa), IX (marine cone snail, 14 kDa) and X (human leukocytes, spleen, thymus, lung, colon and pancreas, 14 kDa) belong to the $sPLA_2$s and groups IV (macrophages, platelets and monocytes, 85 kDa), VI (macrophages, 80–85 kDa) and VIII (bovine brain, 29 kDa) are localized in the cytosol; group IV contains calcium-dependent $cPLA_2$s. PLA_2s catalyze the hydrolysis of the 2-acyl ester bond in 3-*sn*-glycerophospholipids, liberating fatty acids and lysophospholipids. Intermediate enzymes use arachidonic acid (an unsaturated fatty acid) as a substrate for the generation of eicosanoids (for example, leukotrienes, prostaglandins, thromboxanes and other products). These intermediate eicosanoid products play an important role in the inflammatory response and blood platelet aggregation (Clifton & Frank, 1999; Sergey *et al.*, 1997). Thus, the enzyme PLA_2 is of great pharmaceutical interest.

Table 1
Crystal, data-collection and refinement statistics and other relevant geometrical parameters.

Values in parentheses are for the highest resolution shell.

PDB code	2b96
Unit-cell parameters (Å)	$a = b = 46.19$, $c = 102.86$
V_M (Å^3 Da^{-1})	2.2
Z	6
Space group	$P3_121$
Resolution range (Å)	19.6–1.7 (1.76–1.7)
No. of observations	116129
Unique reflections	14435 (1296)
No. of working-set reflections	13708
No. of test-set reflections	727
Cumulative completeness at 1.7 Å (%)	98.9 (91.8)
R_{merge}† (%)	13.2 (43.9)
R_{work} (%)	20.2
R_{free} (%)	22.1
Protein model	
Protein atoms	954
Calcium ions	3
Chloride ion	1
Water O atoms	125
Anisic acid atoms	11
Tris atoms	32
R.m.s. deviation from ideal values	
Bond lengths (Å)	0.006
Bond angles (°)	1.2
Dihedral angles (°)	22.2
Improper angles (°)	0.70
Average atomic temperature factors of the refined model (Å^2)	
Main-chain atoms	18.38
Side-chain atoms	23.23
Water O atoms	41.57
Calcium ions	18.03
Chloride ion	20.06
Anisic acid atoms	31.57
Tris atoms	37.64

† $R_{merge} = \sum_{hkl} |I - \langle I \rangle| / \sum I$, where I is the observed intensity and $\langle I \rangle$ is the average intensity from observations of symmetry-related reflections.

sPLA$_2$s have highly structurally conserved catalytic residues and seven disulfide bonds which play vital roles in maintaining the stability of the structure and function of the enzymes (Dennis, 2000). The calcium ion is an essential cofactor for substrate binding and catalysis (Scott *et al.*, 1990). Several PLA$_2$s have been extracted from the venoms of snakes and bees and from the pancreatic juices of mammals (bovine and porcine). Their three-dimensional crystal structures have been elucidated in recent decades (Scott *et al.*, 1990, 1991; Chandra *et al.*, 2001; Dijkstra *et al.*, 1978, 1981, 1983; Sekar, Sekharudu *et al.*, 1998; Sekar & Sundaralingam, 1999; White *et al.*, 1990). In view of their great pharmacological interest, considerable attention is being devoted towards selecting potential inhibitors/drugs for the enzymes. To this end, many crystal structures with possible inhibitors (for example, tetrahedral mimicking phospholipid molecules, simple organic molecules *etc*.) complexed with PLA$_2$s have been solved (Scott *et al.*, 1990, 1991; White *et al.*, 1990; Cha *et al.*, 1996; Chandra, Jasti, Kaur, Dey *et al.*, 2002; Chandra, Jasti, Kaur, Srinivasan *et al.*, 2002; Chandra, Jasti, Kaur, Betzel *et al.*, 2002; Sekar, Eswaramoorthy *et al.*, 1997; Sekar, Kumar *et al.*, 1998; Sekar *et al.*, 2003; Thunnissen *et al.*, 1990, 1993; Tomoo *et al.*, 1994). Recently, our group solved the crystal structure of a triple mutant (K53,56,120M) of bovine pancreatic PLA$_2$ complexed with anisic acid (Sekar *et al.*, 2003) at 2.6 Å resolution. We noticed that the conserved structural water connecting the interfacial residues Ala1, Pro68, Tyr52 and Asp99 was missing. During our previous investigations of the inhibitor-free structures of other triple mutants K56,120,121M (Rajakannan *et al.*, 2002) and K53,56,121M (Sekar *et al.*, 2005), we observed the presence of a second calcium ion. The idea of the mutation of the residues 53, 56, 120 and 121 from lysine to methionine in the above mutants is to eliminate the anionic interface of the wild type (WT) and to enhance the zwitterionic interface (Yu *et al.*, 2000). Thus, we have investigated the crystal structure of the triple mutant (K53,56,121M) of bovine pancreatic PLA$_2$ complexed with anisic acid to determine whether the inhibitor binds to the second calcium ion (in addition to binding to the primary calcium ion in the active site) and further to probe the missing conserved structural water molecule.

2. Materials and methods

2.1. Crystallization and data collection

The mutant PLA$_2$ was generated by site-directed mutagenesis using the procedure outlined previously (Sekar *et al.*, 2005). The crystals grew within a week at room temperature (293 K) using the hanging-drop vapour-diffusion method from droplets containing 5 µl protein solution (15–20 mg ml^{-1}), 5 m*M* $CaCl_2$, 50 m*M* Tris buffer pH 7.2, 3 µl 60% MPD and 1 µl anisic acid solution. The anisic acid solution was prepared by dissolving the inhibitor (in a eightfold to tenfold molar excess) in the Tris buffer. The reservoir MPD concentration was 70%. For data collection, a crystal of dimensions 0.4 × 0.3 × 0.3 mm was used and the X-ray intensity data were collected at 293 K using our in-house MAR imaging-plate detector. The crystals were trigonal (space group $P3_121$), with unit-cell parameters $a = b = 46.19$, $c = 102.86$ Å (one molecule per asymmetric unit). The intensity data were integrated, scaled and reduced to 1.7 Å resolution using *DENZO* and *SCALEPACK* (Otwinowski & Minor, 1997). A total of 116 129 reflections were collected, which yielded 14 435 unique reflections in the resolution range 19.63–1.7 Å with an R_{merge} of 13.2%. The data completeness in this resolution range was 98.9%. A summary of the data-processing statistics is given in Table 1.

2.2. Structure refinement

The refinement was started using the trigonal form (Sekar, Sekharudu *et al.*, 1998) of the wild type (PDB code 1mkt) using the program *Crystallography and NMR System* (*CNS*) v.1.1 (Brünger *et al.*, 1998). 5% (727 out of 14 435) of the randomly selected (as implemented in *CNS*) reflections were used for the calculation of R_{free} to check the progress of refinement (Brünger, 1992). 25 cycles of rigid-body refinement and 100 cycles of refinement of the atomic positions (Powell energy minimization) lowered the R factor to 32.0% (R_{free} = 33.8%). Subsequently, simulated annealing was performed followed by refinement of the atomic positions and individual

isotropic temperature factors, giving an R factor of 28.6% (R_{free} = 31.2%). The difference electron-density map showed a huge peak (of more than 8σ) in the C-terminal region. Because no chemical other than $CaCl_2$ had been used in crystallization, the huge peak was assigned as a calcium ion based on the neighbouring metal-coordination distances. Furthermore, the difference electron-density map revealed spurious electron density at four different locations. After repeated trials, these peaks were identified as Tris molecules (from the use of Tris buffer in the crystallization) based on the shape of the electron density. The model was fitted into the difference electron-density maps ($2|F_o| - |F_c|$) and ($|F_o| - |F_c|$) using the molecular-graphics program *FRODO* (Jones, 1985). The positions of the inhibitor molecule, three calcium ions, one chloride ion, four molecules of 2-amino-2-hydroxymethyl-1,3-propanediol (Tris) and the three mutated residues at positions 53, 56 and 121 were fitted using difference electron-density maps. 125 water O atoms were identified at various stages of the model building and were included in the refinement. The simulated-annealed omit map was used to check the final protein model. At the end of the refinement, the crystallographic R_{work} and R_{free} were reduced to 20.2 and 22.1%, respectively.

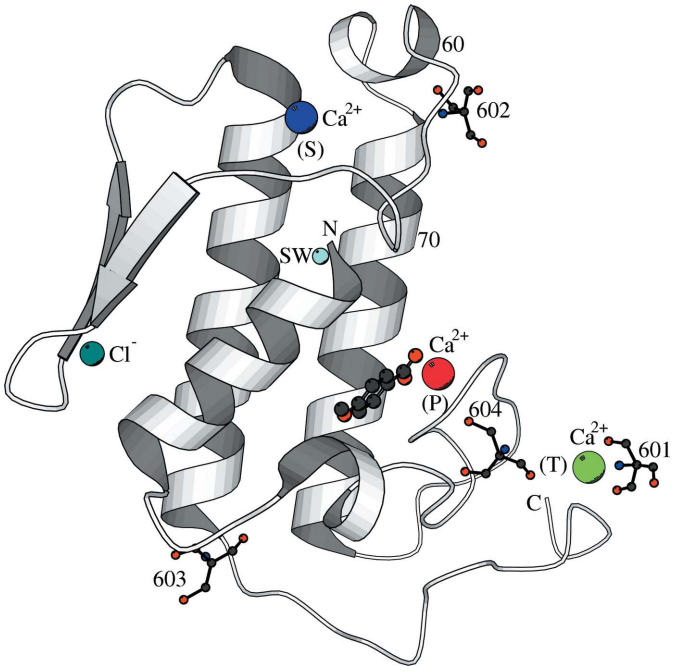

Figure 1
Cartoon diagram of the final model showing the inhibitor (anisic acid) in the active site, three calcium ions [primary (P), second (S) and third (T)], one chloride ion, the structural water molecule (SW) and four Tris molecules (601–604). The surface-loop region (residues 60–70) is also shown.

3. Results and discussion

3.1. Overall structure

The final model contains 123 amino-acid residues (954 atoms), one anisic acid molecule, 125 water O atoms, three calcium ions, one chloride ion and four Tris molecules (Fig. 1). The program *PROCHECK* (Laskowski *et al.*, 1993) was used to check the quality of the final model. All the residues are in the allowed regions of the Ramachandran plot (Ramachandran & Sasisekharan, 1968). 93.6% of the residues are in the most favoured region and the remainder are found in additionally allowed regions. The average coordinate error is estimated to be 0.19 Å by the Cruickshank DPI method (Cruickshank, 1999). A summary of the refined model and relevant geometrical parameters is given in Table 1. The electron density is very clear for all regions of the protein molecule including the inhibitor found in the active site (Fig. 2). Of the 125 water O atoms located, 112 are in the first hydration shell and the remaining 13 are in the second hydration sphere. The remaining three water O atoms make no interaction with any part of the protein molecule and are treated as isolated water molecules. The primary calcium ion found in the active site has seven ligands (five protein atoms, one inhibitor atom and one water molecule). The second calcium ion has six ligands (the side-chain O atoms of Asn71 and Glu92, the main-chain carbonyl O atom of Asn72 and three water O atoms). A chloride ion is also identified at the same position as in the previous cases (Sekar *et al.*, 2004, 2005, 2006; Steiner *et al.*, 2001) and has three ligands. The isotropic temperature factor of the chloride ion is 20 Å^2. Interesting features observed in the present structure are the presence of the third calcium ion, four Tris molecules and the variation in the surface-loop conforma-

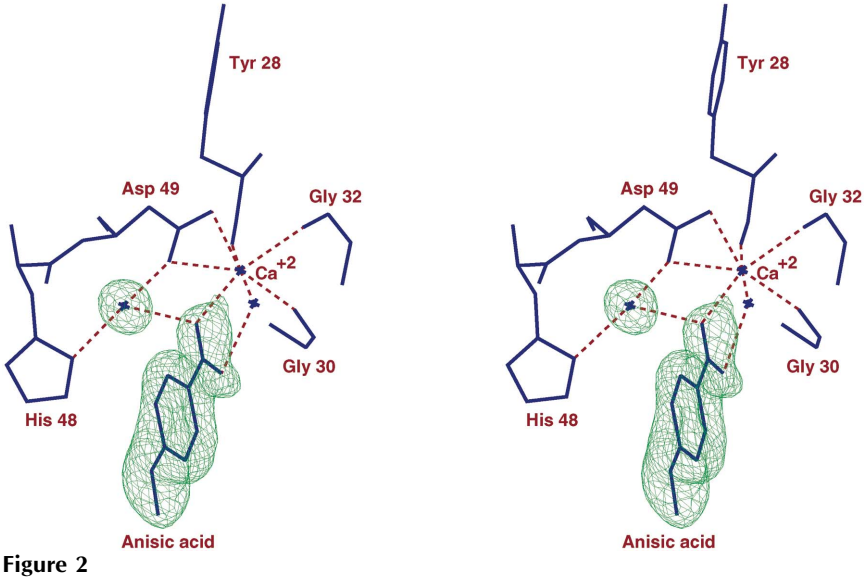

Figure 2
A stereoview of the omit (simulated annealed) electron-density map showing the inhibitor molecule (anisic acid) and its interactions. Contours are shown at 1.0σ.

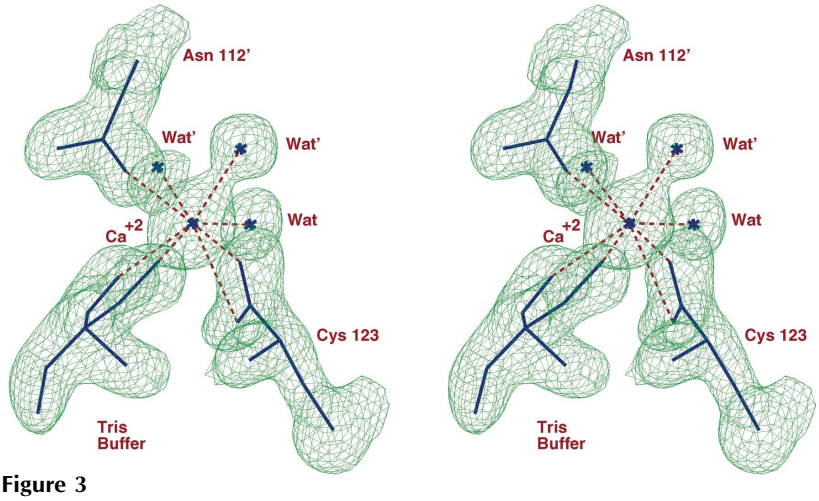

Figure 3
Stereo diagram of the electron-density map contoured at the 1.0σ level showing the third calcium ion and its coordinating ligands.

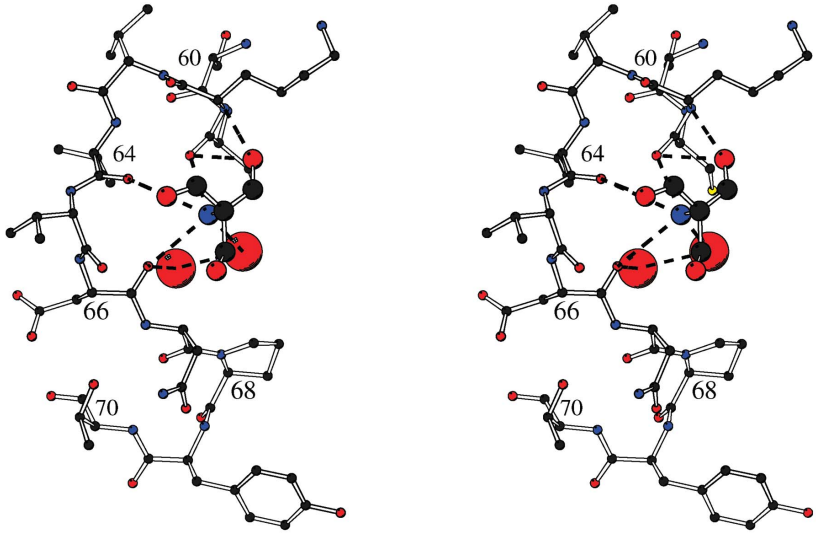

Figure 4
Hydrogen-bonding interactions of Tris molecule 602 with the main-chain atoms of the surface loop. Water molecules are shown as large circles.

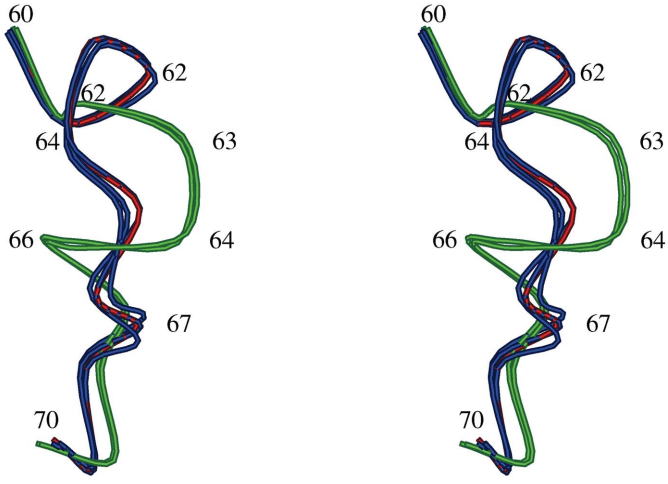

Figure 5
Superposition of the surface-loop residues of the present model (red) with inhibitor-bound structures (blue; PDB codes 1o2e, 1mkv and 1fdk) and structures with a second calcium ion (green; PDB codes 1vl9 and 1gh4).

tion. The roles of these Tris molecules in the coordination of the third calcium ion and the hydrogen-bonding interaction with the surface-loop residues are discussed in detail in the subsequent sections.

3.2. Roles of Tris molecules

This is the first report showing the presence of Tris molecules and their involvement in the structure; these are not present in previously reported structures. A possible reason may be the addition of excess Tris buffer (see §2 for details) in the crystallization droplet. One of the four Tris molecules (601) is identified near the C-terminus. Two O atoms of this molecule are in coordination with the third calcium ion (Fig. 3) at distances of 2.28 and 2.61 Å, respectively (Table 2), and with a water O atom each. Additionally, these coordinating ligands are hydrogen bonded to the carboxyl O atoms of the terminal residue Cys123. Thus, Tris molecule 601 helps in positioning the third calcium ion (see also §3.3 for details). The second Tris molecule (602) is present near the surface loop (residues 60–70). It makes six hydrogen bonds (five hydrogen bonds with the main-chain O atoms and the remainder with the N atom) with the residues in the surface loop (Fig. 4). Furthermore, it also makes hydrogen bonds with the O atom of the mutated residue Met56 and with a water molecule. This strongly suggests that Tris molecule 602 is involved in fixing the conformation of the surface loop. Indeed, the conformation of the surface loop found in the present structure is different from the conformation observed in previous structures where the second calcium ion is present (see also §3.4).

The N1 atom of Tris molecule 603 is found to form hydrogen bonds with the main-chain carbonyl O atoms of Phe106 and Val109 at distances of 3.56 and 2.68 Å, respectively. Furthermore, one of the O atoms (O3) makes hydrogen bonds with the main-chain carbonyl atoms of Phe106 and Val109. In addition, the polar atoms of the Tris molecules make six hydrogen bonds with four water O atoms. Careful examination of previous atomic resolution structures (Sekar *et al.*, 2005; Steiner *et al.*, 2001) reveal the presence of an MPD molecule in the position of the third Tris molecule. The fourth Tris molecule (604) is located near the functionally important primary calcium ion opposite the inhibitor molecule in the active site. The main-chain O atoms of Tyr28, Gly30 and Gly32 from the calcium-binding loop are the natural ligands of the primary calcium ion. Interestingly, one of the O atoms (O1) of the Tris molecule is hydrogen bonded to the main-chain O and N atoms of the residues in the calcium-binding loop. The other O atom (O2) is also involved in hydrogen bonding (Table 2).

Table 2
Interactions of Tris molecules with various protein atoms (interactions with water molecules are not shown).

Tris molecule	Atom	Protein atom	Distance (Å)
601	O1	Third calcium ion	2.28
		123 O	3.30
	O2	123 side-chain O	3.45
		Third calcium ion	2.61
		123 side-chain OT	3.27
	O3	—	
	N1	120 O	3.37
		123 side-chain O	3.23
602	O1	—	—
	O2	64 O	2.90
	O3	56 O	3.21
		61 O	2.98
		62 N	2.86
	N1	61 O	3.28
		64 O	3.52
		66 O	3.31
603	O1	—	—
	O2	—	—
	O3	106 O	2.63
		109 O	2.90
	N1	106 O	3.56
		109 O	2.68
604	O1	28 O†	2.79
		29 O	3.51
		29 N	3.36
		30 O†	2.68
		30 N	3.15
		32 O†	2.75
	O2	25 O	3.03
		25 N	3.16
		26 O	3.09
		29 O	2.58
	O3	—	—
	N1	24 OD1	3.45

† These atoms are the natural ligands of the functionally important primary calcium ion.

3.3. Third calcium ion

As stated previously, this is the first report showing the presence of a third calcium ion in bovine pancreatic PLA_2. Careful examination of the previously reported structures solved in the trigonal space group reveals that a water molecule is located at the position where the third calcium ion is found. In the present structure, this position is identified as a calcium ion since calcium (from $CaCl_2$) was the only metal ion present in the crystallization buffer. It is involved in eight-ligand coordination (Fig. 3) [five ligands from the reference protein molecule (the two terminal O atoms of Cys123, two O atoms from the Tris molecule and one water O atom) and three ligands from the crystallographic symmetry-related molecule (the side-chain O atom of Asn112 and two water O atoms; marked with a prime in Fig. 3)]. The minimum and maximum coordination distances are 2.27 and 2.88 Å, respectively, with an average distance of 2.44 Å. The isotropic temperature factor of the third calcium ion is 19.4 Å^2. The third calcium ion is a distance of 14.59 Å from the primary calcium ion. There are three calcium ions in this structure, each of which exhibits a different coordination number. The functionally important primary calcium ion has seven ligands, the second calcium ion has six ligands and the newly identified third calcium ion has eight ligands. The average isotropic temperature factor of all three calcium ions is 18.0 Å^2. Since the third calcium ion is stabilized *via* the Tris molecule, it is unlikely that this ion is of biological relevance.

3.4. Surface-loop conformation

The residues (60–70) in the surface loop are found to be disordered in most bovine pancreatic PLA_2 structures studied so far (Huang *et al.*, 1996; Sekar, Yu *et al.*, 1997; Sekar, Kumar *et al.*, 1998; Sekar *et al.*, 1999, 2003, 2006; Yu *et al.*, 2000). In the present study, the surface-loop residues are ordered and have clear electron density. The average isotropic temperature factor of all 85 atoms of the surface loop is 23.8 Å^2. Fig. 5 shows a superposition of the residues of the surface loop with the corresponding region in inhibitor-bound structures (PDB codes 1o2e, 1mkv and 1fdk) and in structures containing the second calcium ion (PDB codes 1gh4 and 1vl9). It is found that the conformation of the surface loop is different in the structures where a second calcium (green; Fig. 5) ion is present. In the inhibitor-bound structures, the surface loop is always ordered, as the inhibitor molecule is hydrogen bonded to the phenolic hydroxyl atom of Tyr69. In the case of structures containing the second calcium ion, a hydrogen-bonding network was observed between the surface-loop residues and the water ligands of the second calcium ion. Analysis of the present refined structure reveals the absence of the hydrogen-bonding network. Interestingly, the polar atoms of the Tris molecule (602) provide seven hydrogen bonds (six with O atoms and one with an N atom of the main chain). It is clear from Fig. 5 that the conformation of the surface loop is altered for residues 62–66. However, these residues are stabilized by the hydrogen bonds *via* the Tris molecule (Fig. 4). It suggests that the conformational change observed in the loop can mainly be attributed to the hydrogen bonds provided by the Tris molecule and it is believed that these hydrogen bonds are much stronger compared with the water network between the second calcium ion and the surface-loop residues. Thus, based on these observations, it is tempting to conclude that in the present structure the surface-loop conformation is controlled by the hydrogen bonds *via* the Tris molecule.

3.5. Functional water molecules

There are five structurally and functionally important water molecules (two primary calcium coordination water molecules, two histidine-bound water molecules and a conserved structural water molecule) responsible for the active-site integrity and hydrolytic activity. As found in the previous medium-resolution structure (Sekar *et al.*, 2003), two of these water molecules (the equatorially coordinated water molecule liganded to the primary calcium ion and one of the water molecules which is hydrogen bonded to His48 $N^{\delta1}$) in the active site are replaced by the two carboxylate O atoms of the bound anisic acid molecule. In contrast to our previous study (Sekar *et al.*, 2003), the conserved structural water molecule

that stabilizes the interfacial recognition site residues Ala1, Pro68, Tyr52 and Asp99 is observed in the present model.

4. Conclusions

The three-dimensional crystal structure of the triple mutant complexed with an organic molecule (anisic acid) has been refined at 1.7 Å resolution. An interesting observation is that the surface-loop residues are ordered and the overall conformation is different compared with that of structures in which a second calcium ion is present. Indeed, the surface-loop conformation is controlled by the Tris molecule. The second feature is the presence of the third calcium ion near the C-terminus and this is again anchored by another Tris molecule. In contrast to our expectation, the inhibitor molecule is not seen bound to the second calcium ion (near the surface loop) even though there is sufficient space to accommodate it. The conserved structural water molecule is present in the structure.

X-ray diffraction data were collected at the National Data Collection Facility for Structural Biology supported by the Department of Science and Technology (DST) and the Department of Biotechnology (DBT), Government of India. Use of the facilities at the Supercomputer Education and Research Centre, Bioinformatics Centre and Interactive Graphics Facility (the latter two supported by the DBT) is acknowledged. DV and DG thank the University Grants Commission (UGC) for financial support. KS and DV thank Nagoya University for the visiting professorship under the VBL programme. The work from the laboratory of M-DT is supported by NIH grant GM 57568 and by the Genomics Research Center.

References

Brünger, A. T. (1992). *Nature (London)*, **355**, 472–474.
Brünger, A. T., Adams, P. D., Clore, G. M., DeLano, W. L., Gros, P., Gross-Kunstleve, R. W., Jiang, J.-S., Kuszewski, J., Nilges, M., Pannu, N. S., Read, R. J., Rice, L. M., Simonson, T. & Warren, G. L. (1998). *Acta Cryst.* D**54**, 905–921.
Cha, S. S., Lee, D., Adams, J., Kurdyla, J. T., Jones, C. S., Marshall, L. A., Bolognese, B., Abdel-Meguuid, S. S. & Oh, B.-H. (1996). *J. Med. Chem.* **39**, 3878–3881.
Chandra, V., Jasti, J., Kaur, P., Betzel, C., Srinivasan, A. & Singh, T. P. (2002). *J. Mol. Biol.* **320**, 215–222.
Chandra, V., Jasti, J., Kaur, P., Dey, S., Srinivasan, A., Betzel, C. & Singh, T. P. (2002). *Acta Cryst.* D**58**, 1813–1819.
Chandra, V., Jasti, J., Kaur, P., Srinivasan, A., Betzel, C. & Singh, T. P. (2002). *Biochemistry*, **41**, 10914–10919.
Chandra, V., Kaur, P., Jasti, J., Betzel, C. & Singh, T. P. (2001). *Acta Cryst.* D**57**, 1793–1798.
Clifton, O. B. & Frank, K. A. (1999). *Proc. Assoc. Am. Phys.* **111**, 516–517.
Cruickshank, D. W. J. (1999). *Acta Cryst.* D**55**, 583–601.
Dennis, A. E. (2000). *Am. J. Respir. Crit. Care Med.* **161**, S32–S35.
Dijkstra, B. W., Drenth, J., Kalk, K. H. & Vandermaelen, P. J. (1978). *J. Mol. Biol.* **124**, 53–60.
Dijkstra, B. W., Kalk, K. H., Hol, W. G. J. & Drenth, J. (1981). *J. Mol. Biol.* **147**, 97–123.
Dijkstra, B. W., Renetseder, R., Kalk, K. H., Hol, W. G. J. & Drenth, J. (1983). *J. Mol. Biol.* **168**, 163–179.
Huang, B., Yu, B. Z., Rogers, J., Byeon, I. J., Sekar, K., Chen, X., Sundaralingam, M., Tsai, M.-D. & Jain, M. K. (1996). *Biochemistry*, **35**, 12164–12174.
Jones, T. A. (1985). *Methods Enzymol.* **115**, 157–171.
Laskowski, R. A., MacArthur, M. W., Moss, D. S. & Thornton, J. M. (1993). *J. Appl. Cryst.* **26**, 283–291.
Otwinowski, Z. & Minor, W. (1997). *Methods Enzymol.* **276**, 307–|326.
Rajakannan, V., Yogavel, M., Poi, M.-J., Jeyaprakash, A. A., Jeyakanthan, J., Velmurugan, D., Tsai, M.-D. & Sekar, K. (2002). *J. Mol. Biol.* **324**, 755–762.
Ramachandran, G. N. & Sasisekharan, V. (1968). *Adv. Protein Chem.* **23**, 283–438.
Scott, D. L., White, S. P., Browning, J. L., Rosa, J. J., Gelb, M. H. & Sigler, P. B. (1991). *Science*, **254**, 1007–1010.
Scott, D. L., White, S. P., Otwinowski, Z., Yuan, W., Gelb, M. H. & Sigler, P. B. (1990). *Science*, **250**, 1541–1546.
Sekar, K., Biswas, R., Li, Y., Tsai, M.-D. & Sundaralingam, M. (1999). *Acta Cryst.* D**55**, 443–447.
Sekar, K., Eswaramoorthy, S., Jain, M. K. & Sundaralingam, M. (1997). *Biochemistry*, **36**, 14186–14191.
Sekar, K., Kumar, A., Liu, X. H., Tsai, M.-D., Gelb, M. H. & Sundaralingam, M. (1998). *Acta Cryst.* D**54**, 334–341.
Sekar, K., Rajakannan, V., Gayathri, D., Velmurugan, D., Poi, M.-J., Dauter, M., Dauter, Z. & Tsai, M.-D. (2005). *Acta Cryst.* F**61**, 3–7.
Sekar, K., Rajakannan, V., Velmurugan, D., Yamane, T., Thirumurugan, R., Dauter, M. & Dauter, Z. (2004). *Acta Cryst.* D**60**, 1586–1590.
Sekar, K., Sekharudu, C., Tsai, M.-D. & Sundaralingam, M. (1998). *Acta Cryst.* D**54**, 342–346.
Sekar, K. & Sundaralingam, M. (1999). *Acta Cryst.* D**55**, 46–50.
Sekar, K., Vaijayanthi Mala, S., Yogavel, M., Velmurugan, D., Poi, M.-J., Vishwanath, B. S., Gowda, T. V., Jeyaprakash, A. A. & Tsai, M.-D. (2003). *J. Mol. Biol.* **333**, 367–376.
Sekar, K., Yogavel, M., Gayathri, D., Velmurugan, D., Krishna, R., Poi, M.-J., Dauter, Z., Dauter, M. & Tsai, M.-D. (2006). *Acta Cryst.* F**62**, 1–5.
Sekar, K., Yu, B.-Z., Roger, J., Lutton, J., Liu, X., Chen, X., Tsai M.-D., Jain, M. K. & Sundaralingam, M. (1997). *Biochemistry*, **36**, 3101–3114.
Sergey, S., Sergei, I. & Klaus, S. (1997). *J. Mol. Model.* **3**, 473–475.
Steiner, R. A., Rozeboom, H. J., de Vries, A. A., Kalk, K. H., Murshudov, G. N., Wilson, K. S. & Dijkstra, B. W. (2001). *Acta Cryst.* D**57**, 516–526.
Thunnissen, M. M. G. M., Eiso, A. B., Kalk, K. H., Drenth, J., Dijkstra, B. W., Kuipers, O. P., Dijkman, R., de Haas, G. H. & Verheij, H. M. (1990). *Nature (London)*, **347**, 689–691.
Thunnissen, M. M. G. M., Franken, P. A., de Haas, G. H., Drenth, J., Kalk, K. H., Verheij, H. M. & Dijkstra, B. W. (1993). *J. Mol. Biol.* **232**, 839–855.
Tomoo, K., Ohishi, H., Ishida, T., Inoue, M., Ikeda, K., Sumiya, S. & Kitamura, K. (1994). *Proteins*, **19**, 330–339.
White, S. P., Scott, D. L., Gelb, M. H. & Sigler, P. B. (1990). *Science*, **250**, 1560–1563.
Yu, B.-Z., Poi, M.-J., Ramagopal, U. A., Jain, R., Ramakumar, S., Berg, O. G., Tsai, M.-D., Sekar, K. & Jain, M. K. (2000). *Biochemistry*, **39**, 12312–12323.